Organometallics 1990, 9, 1806–1812

at 546 nm, also supporting the dissociative nature of the process. This observation is also in line with the resonance Raman data referred to before,[13,14] according to which the *cis*-metal–carbonyl bond is partially labilized during MLCT excitation, thus enabling the dissociative reaction mode. The labilization is obviously less than in the case of LF excitation as seen from the $\Delta V^{\ddagger}$ value of +2.7 cm^3 mol^{-1} as compared to +9.6 cm^3 mol^{-1} in the latter case. On the basis of this difference, we can also exclude the possibility of a reaction via back population of the LF excited state, since then the observed volume of activation should be larger than for the LF substitution process. LF excited states in general have a higher partial molar volume than MLCT states,[7,37] and this volume difference will then have to add on to the volume of activation for the LF substitution process. Such a situation was reported recently for the photosubstitution reactions of a series of $W(CO)_5$(4-X-pyridine) (X = H, acetyl, cyano) complexes, where the introduction of an electron-withdrawing group initiates MLCT excitation.[37] The unsubstituted pyridine (X = H) complex undergoes dissociative LF photosubstitution for which $\Delta V^{\ddagger}$ is +5.6 cm^3 mol^{-1}, whereas the substituted pyridine complexes undergo partial MLCT excitation followed by back population of the LF excited state. The observed $\Delta V^{\ddagger}$ in the latter case is larger than reported for the unsubstituted complex, viz. +6.3 (X = cyano) and +9.9 (X = acetyl) cm^3 mol^{-1}. It is therefore likely that $Cr(CO)_4$phen undergoes dissociative photosubstitution from both the LF and MLCT excited states. The absolute magnitude of $\Delta V^{\ddagger}$ suggests a D mechanism in the former and I_d mechanism in the latter case, since less M–CO bond weakening is expected to occur during MLCT excitation as compared to LF excitation. Alternatively, the low $\Delta V^{\ddagger}$ found at 546 nm could be due to a combination of both (MLCT and LF) reaction paths. In this respect it is interesting to note that a limiting quantum yield was also found at high wavelengths for the photosubstitution of $Cr(CO)_4$(bipyridine), which presumably also points to a reaction occurring from the CT excited state.[39]

The significantly different $\Delta V^{\ddagger}$ values reported in this study for LF and CT photosubstitution of $Mo(CO)_4$phen and $W(CO)_4$phen clearly underline the different substitution mechanisms operating from these excited states and support earlier arguments in favor of the photoactivity of the MLCT states in such complexes.[13,14,16] The results furthermore underline the value of pressure as a key parameter to distinguish between associative and dissociative photosubstitution mechanisms. Mechanistic interpretation in terms of partial molar volume changes is more straightforward than in terms of energy changes, i.e., a volume profile treatment versus an energy profile treatment.

Acknowledgment. We gratefully acknowledge financial support from the Deutsche Forschungsgemeinschaft, Fonds der Chemischen Industrie, and Volkswagen-Stiftung, as well as a DAAD fellowship to K.B.R.

---

[39] Vlcek, A., Jr.; Hartl, F. *Photochem. Symp. Smolenice (SOPTROCC 6)*, 1988.

Synthesis and X-ray Structure of an (Oxodimethylidenemethane)iron Dimer, $[(CH_2COCH_2)(CO)_3Fe]_2$

Markus Frey,[†] Titus A. Jenny,*[,†] and Helen Stoeckli-Evans[‡]

Institut de chimie organique, University of Fribourg, Fribourg, Switzerland, and Insitut de chimie, University of Neuchâtel, Neuchâtel, Switzerland

Received October 18, 1989

An iron carbonyl π-complex of the oxyallyl species was synthesized in two steps by complexation of a silylenol ether of α-bromoacetone and subsequent dehydrohalogenation by pyridine/$AgBF_4$. The isolated intermediate, bromotricarbonyl(η^3-2-hydroxy-2-propenyl)iron, shows an unexpectedly high acidity (pK_a = 5.2). The tricarbonyl(oxyallyl)iron complex exists as $[(CH_2COCH_2)(CO)_3Fe]_2$ only, a head-to-tail dimer, as revealed by ^1H and ^{13}C NMR spectroscopy as well as by X-ray diffraction analysis. This complex shows a butterfly like bent skeleton of C_2 symmetry which inverts on the NMR time scale with an activation energy of 72 kJ/mol at room temperature. It crystallizes as orange hexagonal plates in the orthorhombic space group $Pbc2_1$ with a = 11.658 (2) Å, b = 6.192 (1) Å, c = 20.311 (4) Å, and Z = 4. According to the analytical and chemical observations, this complex exhibits a structure halfway between a 2-substituted π-allylic complex and a metallacyclobutanone compound.

Introduction

Oxyallyl **1** has always intrigued chemists from both a theoretical[1] and a synthetic[2] point of view, as a still-elusive species, which may however be involved as a short-lived intermediate in well-known reactions like the Faworski rearrangement and the Noyori cycyloaddition. Cyclopropanone **2**, stable itself only in solution at low temperatures, and allene oxide **3**, unknown without stabilizing substituents, have been referred to as limiting structures of oxyallyl, based on one hand on calculated energies[1a,3] of the molecules and their interconversion barriers and on the other hand on reaction product analyses.[4]

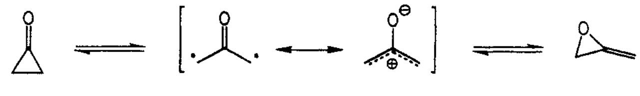
2 1 3

The evident similarity of oxyallyl and trimethylidenemethane **4** (TMM) prompted us to attempt a stabilization of the species by complexation with a suitable transition

---

[†] University of Fribourg.

[‡] University of Neuchâtel.

[1] (a) Osamura, Y.; Borden, W. T.; Morokuma, K. *J. Am. Chem. Soc.* **1984**, *106*, 5112. (b) Lahti, P. M.; Rossi, A. R.; Berson, J. A. *J. Am. Chem. Soc.* **1985**, *107*, 2273.

[2] For a recent review, see: Mann, J. *Tetradedron*, **1986**, *42*, 4611.

[3] (a) Sevin, A.; Fazilleau, E.; Chaquin, P. *Tetrahedron* **1981**, *37*, 3831. (b) Ortiz, J. V. *J. Org. Chem.* **1983**, *48*, 4744.

[4] Edelson, S. S.; Turro, N. J. *J. Am. Chem. Soc.* **1970**, *92*, 2770.

0276-7333/90/2309-1806$02.50/0

Table I. Substitution Dependence of Cycloaddition Yields of Different Oxyallyl Precursors

	R_1	R_2	X	% yield 22	ref
2a	H	H		0	
b	H	CH_3		$\sim100^a$	9
c	CH_3	CH_3		100	
11b	H	H	Cl	6^b	
c	H	CH_3	Br	50	
d	CH_3	CH_3	Br	97	10
16a	H	H	Cl	0	
b	H	CH_3	Cl	5	11
c	CH_3	CH_3	Cl	66	

[a] No yield given explicitly. [b] Accompanied by 6% 1-(2-furanyl)-propan-2-one.

metal, e.g., iron, to obtain the hetero analogue of (TMM)Fe(CO)$_3$ **5**, namely, (oxodimethylidenemethane)-

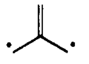

4

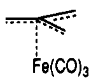

5

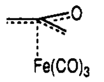

6

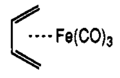

7

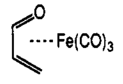

8

Fe(CO)$_3$ **6**. Replacement of one carbon atom in the π-bonded system of olefinic ligands by an oxygen atom is normally tolerated by iron, exemplified[5] by the pair of compounds (butadiene)Fe(CO)$_3$ (**7**) and (acrolein)Fe(CO)$_3$[6] (**8**).

Although complex **6** might be formed transitionaly, it rapidly dimerizes in solution to be isolated only in the form of the oxyallyl complex **9**. This type of dimer is not known for the analogous TMM complex **5** but has been proposed[7] for the somehow related dimeric iron complex **10a** of cyclopentadienone.

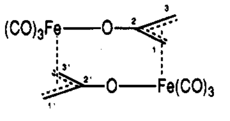

9

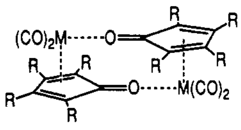

10a M = Fe, R = H
10b M = Ru, R = Ph

Results and Discussion

Synthesis. The title compound, **9**, was synthesized by first complexing the known[8] α-bromosilylenolate **11a** with nonacarbonyldiiron (Fe$_2$(CO)$_9$) to obtain the desilylated allylic complex **13a**, which was subsequently dehydrobrominated with a pyridine/silver tetrafluoroborate (AgBF$_4$) complex (Scheme I and Table I). Both the bromo (**11a**) and the chloro derivatives (**11b**) yielded the corresponding alylic complexes **13a** and **13b** as the only isolatable product, although in the bromo case the yield was considerably higher.

Scheme I[a]

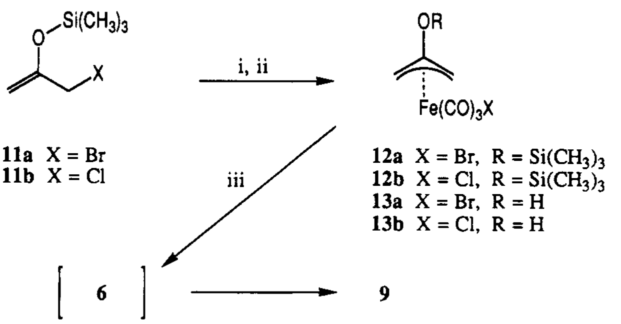

[a] (i) Fe$_2$(CO)$_9$ in benzene; (ii) silica gel; (iii) Ag(BF$_4$)/pyridine (1:1) in diethyl ether.

Scheme II

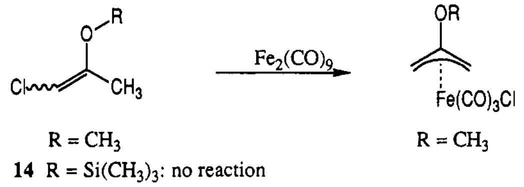

Attempts to synthesize **13b** starting from 1-chloro-2-[(trimethylsilyl)oxy]propene (**14**), as suggested in analogy to the reported[12] behavior of the corresponding methoxy derivatives (Scheme II), turned out to be unsuccessful since **14** does not react with Fe$_2$(CO)$_9$.

Surprisingly, the trimethylsilyl protecting group became extremely labile in the complexes **12a** and **12b**: the crude reaction mixture after complexation of the corresponding silylenol ethers with Fe$_2$(CO)$_9$ always contained both the silylated and desilylated products in variing proportions. These mixtures were conveniently converted to the desilylated product during chromatography on silica gel. This finding is paralleled by the high acidity of the hydroxyl group in **13a**. Potentiometric titration with 0.1 M NaOH in 48% (w/w) aqueous ethanol[13] yielded a pK_a value of 5.9, corresponding to a pK_a value of 5.2 in water.

The dehydrohalogenation of the allylic complex **13a** was achieved by concomitant deprotonation and dehalogenation with a previously prepared 1:1 precipitate of pyridine and AgBF$_4$ in diethyl ether. This procedure guaranteed a low concentration of both free pyridine and silver ions throughout the reaction. Consecutive exposure of the allylic complexes to either sequence of the same reagents resulted in rapid degradation and formation of acetone[14] as the only isolable product. Although the complexes **13a** and **13b**, air stable in the solid state, do not decompose in oxygen-free solutions at room temperature, the corresponding anions rapidly degrade even at lower temperatures with an estimated lifetime of 2 h. Complex **9**, moderately air stable in the solid state, slowly decomposes in oxygen-free solutions, preventing thereby any high-resolution NMR analysis.

To trap the proposed intermediate complex **6** in a cycloaddition reaction, the above dehydrohalogenation reaction was carried out in furan as the solvent. No 8-oxabicyclo[3.2.1]oct-6-en-3-one[15] (**15a**) was found, however.

---

(5) Similar pairs of substituted complexes are well-known in literature.

(6) Sorriso, S.; Cardaci, G. *J. Organomet. Chem.* **1975**, *101*, 107.

(7) Mays, M. J.; Morris, M. J.; Raithby, P. R.; Shvo, Y.; Czarkie, D. *Organometallics* **1989**, *8*, 1162, and references therein.

(8) Hosomi, A.; Shirahata, A.; Araki, Y.; Sakurai, H. *J. Org. Chem.* **1981**, *46*, 4631.

(9) Turro, N. J.; Edelson, S. S.; Williams, J. R.; Darling, T. R.; Hammond, W. B. *J. Am. Chem. Soc.* **1969**, *91*, 2283.

(10) Sakurai, H.; Shirahata, A.; Hosomi, A. *Angew. Chem., Int. Ed. Engl.* **1979**, *91*, 163.

(11) Herter, R.; Foehlisch, B. *Synthesis* **1982**, 976.

(12) Hill, A. E.; Hoffmann, H. M. R. *J. Chem. Soc., Chem. Commun.* **1972**, 574.

(13) De Puy, C. H.; Greene, R. N.; Schroer, T. E. *J. Chem. Soc., Chem. Commum.* **1968**, 1225.

(14) Yield up to 27% as determined by ^{1}H NMR using an internal standard.

(15) Hill, A. E.; Greenwood, G.; Hoffman, H. M. R. *J. Am. Chem. Soc.* **1973**, *95*, 1338.

Table II. NMR Data of Oxygen-Substituted Allyl Iron Complexes

compd			^1H NMR (δ, ppm; $J_{H,H}$, Hz)					^{13}C NMR (δ, ppm)[a]			
	R	X	$\delta_{H_{syn}}$	$\delta_{H_{anti}}$	$^2J_{as}$	$^4J_{ss'}$	$^4J_{as'}$	C(1,3)	C(2)	CO_{ap}	CO_{eq}
13a	H	Br	3.29	3.10	4.01	3.51	0.08	51.4	148.1	207.0	206.5
	(anion)	Br	4.08	3.50	3.51	3.69	0.12				
	CH_3	Br	3.60	3.14	4.29	3.78	0.05				
13b	H	Cl	3.37	2.98				54.3	148.1	204.7	205.2
12b	$Si(CH_3)_3$	Cl	3.90	3.25	3.10	3.50	0.10				
9	(dimer)[b]		2.77	1.70	*d*	*d*	*d*	44.6	168.0	209.6	207.9
9	(dimer)[c]		2.88[e]	2.36				48.8	168.0	209.1	208.1
				1.95				39.5			207.0

[a] The atomic numbering is given with formula **9**. [b] C_6D_6, 298 K. [c] CD_2Cl_2, 223 K. [d] Not resolved. [e] Broad resonance.

Scheme III[a]

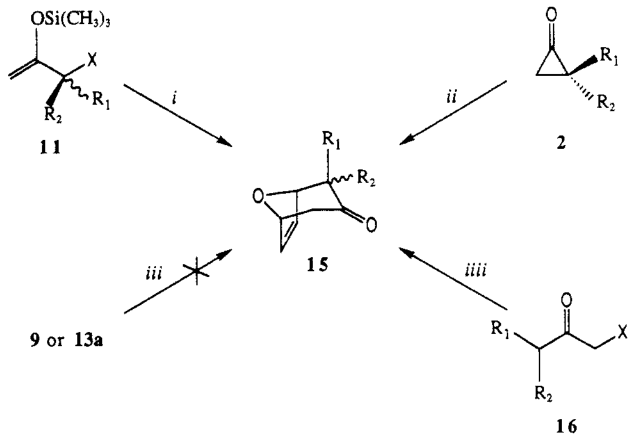

[a] (i) CH_2Cl_2, furan, $ZnCl_2$; (ii) CH_2Cl_2, furan; (iii) furan, heat; (iiii) diethyl ether, furan, NEt_3, $LiClO_4$.

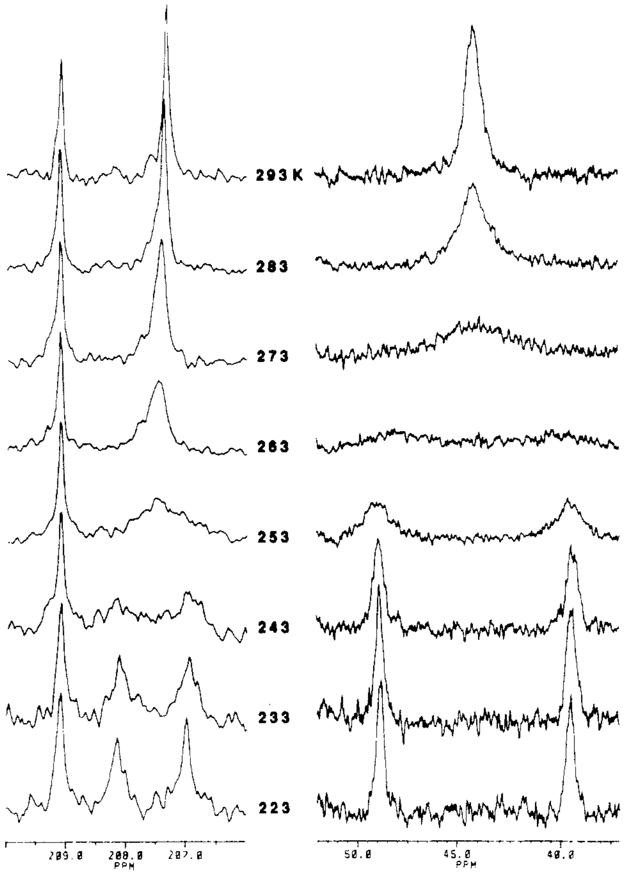

Figure 1. Variable-temperature ^{13}C NMR spectra of [tricarbonyl(oxodimethylidenemethane)iron]dimer **9** in CD_2Cl_2 solution; carbonyl and aliphatic region.

Hence the reaction rate for cycloaddition is too small compared to the dimerization of **6**. Attempts to generate **6** by pyrolysis of either **9** or **13a** and trapping it by cocondensation with furan onto a coldfinger were unsuccessful. This cannot be due to difficulties in bringing the starting materials into the gas phase, since the compounds easily vaporize as shown by the high ion yield in the mass spectrometer at source temperatures above 110 °C.

The lack of reactivity of the unsubstituted oxyallyl complex is paralleled by the low tendency for cycloaddition of the corresponding uncomplexed oxyallyl, e.g., prepared from silylenol ethers **11**, cyclopropanones **2**, or α-haloketones **16** (Scheme III). Cycloaddition products are observed only in low yield in the case of **11c**. The reactivity toward cycloaddition is greatly increased by substituents as shown in Table I. This might be due to an enhanced stabilization of the zwitterionic intermediate oxyallyl species. Whether the same conclusion also applies for the case of π-complexed oxyallyl is under current investigation.

Spectroscopic Data. Table II summarizes the relevant ^1H and ^{13}C NMR data. Typicaly, AA′XX′ patterns were observed for the ^1H NMR signals of the CH_2 groups of the allylic ligands in all complexes. The degenerate form of the multiplets (six lines observed only) points to a zero (or near zero) J_X coupling constant. It was assigned to the coupling between the anti[16] hydrogens, whereas the larger J_A coupling constant ranging from 3.5 to 3.8 Hz nicely fits the W-shaped coupling path between the syn hydrogens. A more pronounced dependence on variations at the oxygen substituent appears for the geminal coupling: the value increases by 40% in going from a trimethylsilyl to a methyl substitution. The assignment of the J_A and J_X coupling constants respectively was confirmed for the case of **13a** through the observation and analysis of the first-order side bands of the $^{13}C(1)$ isotopomer in the ^1H NMR spectrum. Unfortunately, the achievable resolution in the case of the dimeric complex **9**, due to slow decomposition in solution, did not allow for an adequate analysis. Nevertheless, characteristic spectral changes occur for this compound: it shows by far the lowest chemical shifts for the syn and anti hydrogens, concomitantly with the largest shift difference (1.07 ppm), in the whole series. Unambiguous assignment of the syn and the anti hydrogens in **13a** was made possible through the different amount of induced shifts upon addition of $Eu(fod)_3$, i.e., a 2.2-fold larger displacement for the signal at 4.25 ppm (H_{syn}) compared to the signal at 3.36 ppm (H_{anti}) was noted. The same relative chemical shift sequence was assumed for all other cases, in agreement with the general assignment found in the literature for complexes with allylic ligands substituted at the central carbon.

The ^{13}C NMR spectrum of **9** revealed the presence of a hindered movement in the molecule, since the signals for

---

[16] Deeming, A. J. in *Comprehensive Organometallic Chemistry*; Wilkinson, G., Stone, F. G. A., Abel, E. W., Eds.; Pergamon Press: Oxford, 1982; Vol. 4, p 413.

Table III. π-Allylmetal and Metallacyclobutanone Folding Angle and $^1J_{C,H}$ Coupling Constants

compd	folding angle, deg	$^1J_{C,H}$, Hz	hybridization sp^x,[17] x
9	60.4, 60.7	153	2.33
13a		165, 157.5[a]	2.11, 2.24
13b		167, 158[a]	2.07, 2.23
17	68.7	164, 161[a]	2.13, 2.18
18	53.3	156.4, 151.2[a]	2.26, 2.36
19	40.7	146.2	2.46

[a] Coupling constants with syn and anti proton, respectively.

the terminal carbon atoms of the two allylic moieties appear as a single broad line at room temperature. Lowering the temperature resulted in a splitting into two lines both of this signal and of one of the signals attributed to the carbonyl ligands (Figure 1). From a line-shape analysis the activation enthalpy $\Delta H^{\ddagger} = 70 \pm 5$ kJ/mol and activation entropy $\Delta S^{\ddagger} = 85 \pm 20$ J/mol·K were deduced. This behavior is paralleled by the ^1H NMR spectrum: the AA′XX′ pattern observed at room temperature changes into a ABMX system, although the AB part therein remains unresolved even at the lowest accessible temperature (cf. Table II). Evidently, the C_{2h} symmetry found in the ruthenium complex **10b**[7] is reduced to C_2 in our case, as suggested by inspection of molecular models: a flat ring[17] would require completely bent-away allylic ligands in order to allow for normal bond angles (ca. 130°) at the bridging oxygen atoms. We therefore attribute the observed fluctionality to a ring inversion process between the two degenerative, enantiomeric C_2 boat conformations of **9**. This analysis of the behavior of **9** in solution was fully confirmed by the observed C_2 structure in the solid state (vide infra discussion of the X-ray analysis).

The measured ^{13}C NMR chemical shifts and $^1J_{C,H}$ coupling constants (cf. Tables II and III) require some additional commentary. The chemical shift for C(2) in **13a** lies in the expected range[18] 135–150 ppm. Surprisingly, the signal of the corresponding carbon in **9** is downfield shifted by 20 ppm, compared to **13a**, whereas a high-field shift of about 10 ppm would be predicted. One possible explanation may be found in an increased participation of the limiting structure **9B**.

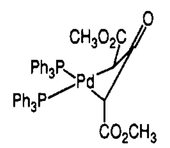

18

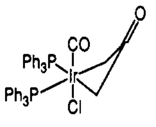

19

Additional evidence is gained through the comparison of the $^1J_{C,H}$ coupling constants at the terminal carbons (C(1,3)) found in our compounds with those of typical allylic ((η^3-C_3H_5)Fe(CO)$_3$Br, **17**[19]) and metallacyclobutanone structures (palladium complex **18**[20] and iridium complex **19**[21]). With use of Newton's semiempirical formula,[22] these $^1J_{C,H}$ coupling constants correspond neither to truly sp^2- nor to sp^3-hybridized carbons, but a clearcut trend from sp^2 toward sp^3 values is noted in going from the allylic complex **17** to the iridacyclobutanone **19**. In conclusion, a mesomeric description of these oxygen-substituted allylic iron complexes, involving both π-complexed η^3-allyl ligands (A) *and* metallacyclobutanones (B) as limiting structures, seems to be more appropriate.

Table IV. Final Positional and Equivalent Isotropic Thermal Parameters [×10^4] with Estimated Standard Deviations in Parentheses ($U_{eq} = {}^1/_3\Sigma\Sigma U_{ij}a_i^*a_j^*[\bar{a}_i \bullet \bar{a}_j]$)

atom[a]	x/a	y/b	z/c	U_{eq}, Å^2
Fe(1)	7415.5 (6)	494.6 (10)	364.0 (4)	388 (2)
O(1)	6815 (3)	1930 (5)	1822 (2)	420 (10)
C(1)	7208 (4)	2600 (8)	1271 (2)	432 (14)
C(2)	8364 (4)	2387 (8)	1042 (3)	442 (14)
C(3)	6427 (5)	3115 (8)	747 (3)	525 (16)
O(4)	8172 (5)	3380 (6)	−681 (2)	836 (18)
C(4)	7892 (5)	2238 (9)	−268 (3)	546 (16)
O(5)	5544 (4)	−1104 (10)	−477 (2)	1027 (20)
C(5)	6268 (5)	−496 (9)	−161 (3)	569 (18)
O(6)	9282 (4)	−2575 (8)	68 (3)	769 (16)
C(6)	8554 (5)	−1418 (8)	184 (2)	486 (16)
Fe(2)	7405.7 (5)	−150.1 (10)	2493.6 (4)	371 (2)
O(21)	6688 (3)	−1403 (5)	1033 (2)	422 (9)
C(21)	7055 (4)	−2177 (6)	1587 (2)	423 (14)
C(22)	8207 (4)	−2269 (8)	1798 (3)	446 (15)
C(23)	6233 (4)	−2506 (9)	2109 (3)	497 (14)
O(24)	7982 (5)	−3281 (8)	3503 (2)	841 (18)
C(24)	7763 (5)	−2040 (9)	3114 (3)	519 (16)
O(25)	5710 (4)	2015 (9)	3344 (2)	900 (19)
C(25)	6352 (5)	1161 (10)	3023 (3)	521 (16)
O(26)	9426 (3)	2498 (9)	2792 (3)	746 (14)
C(26)	8646 (4)	1513 (8)	2675 (2)	473 (15)

[a] Arbitrary numbering scheme (see Figure 2). Crystal data: formula $C_{12}H_8Fe_2O_8$ fw 391.7, orthorhombic system, space group $Pbc2_1$, $a = 11.658$ (2) Å, $b = 6.192$ (1) Å, $c = 20.311$ (4) Å, $V = 1466.2$ Å^2, $F(000) = 784$, $Z = 4$, $D_x = 1.775$ g cm^{-3}, Mo Kα, λ = 0.71073 Å, μ = 20.1 cm^{-1}.

Table V. Selected Bond Distances (Å)

Fe(1)–O(21)	1.987 (3)	Fe(2)–O(1)	1.999 (3)
Fe(1)–C(1)	2.269 (5)	Fe(2)–C(21)	2.267 (4)
Fe(1)–C(2)	2.119 (5)	Fe(2)–C(22)	2.143 (5)
Fe(1)–C(3)	2.137 (5)	Fe(2)–C(23)	2.147 (5)
Fe(1)–C(4)	1.768 (6)	Fe(2)–C(24)	1.770 (5)
Fe(1)–C(5)	1.817 (5)	Fe(2)–C(25)	1.823 (5)
Fe(1)–C(6)	1.816 (5)	Fe(2)–C(26)	1.813 (5)
C(1)–O(1)	1.279 (6)	C(21)–O(21)	1.294 (6)
C(1)–C(2)	1.432 (7)	C(21)–C(22)	1.411 (7)
C(1)–C(3)	1.436 (7)	C(21)–C(23)	1.444 (7)
C(4)–O(4)	1.143 (7)	C(24)–O(24)	1.131 (7)
C(5)–O(5)	1.125 (7)	C(25)–O(25)	1.125 (7)
C(6)–O(6)	1.136 (6)	C(26)–O(26)	1.120 (6)
Fe(1)···Fe(2)	4.3447 (1)	O(1)···O(21)	2.617 (5)
Fe(1)···O(1)	3.170 (4)	Fe(2)···O(21)	3.178 (4)

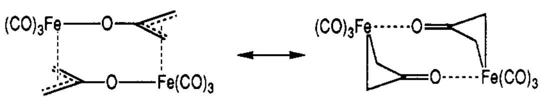

9 A **9 B**

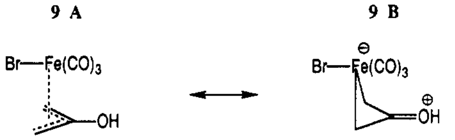

13a A **13a B**

The iron complexes **9**, **13a**, and **13b** yield typical mass spectra on EI ionization, showing subsequent loss of CO ligands. In addition, fragments from a loss of the halogen atom X *and* HX are noted for both the compounds **13a** and **13b**. The mass spectra therefore indicate a facile thermal fragmentation to yield by loss of HX the monomeric complex **6** (m/z 196), since the proportion of the fragments of **13a** or **13b** and **6**, respectively, vary only with

---

(17) A six-membered heterocyclic ring is constituted by the two iron nuclei, the bridging oxygens, and the central carbon atoms of the allylic ligands.

(18) Considering shift increments of oxy and hydroxy substituents in related organic and metallorganic compounds.

(19) Simon, F. E.; Lauher, J. W. *Inorg. Chem.* **1980**, *19*, 2338.

(20) Kemmitt, R. D. W.; McKenna, P.; Russell, D. R.; Sherry, L. J. S. *J. Chem. Soc., Dalton Trans.* **1985**, 259.

(21) Jones, M. D.; Kemmitt, R. D. W.; Fawcett, J.; Russel, D. R. *J. Chem. Soc., Chem. Commun.* **1986**, 427.

(22) Newton, M. D.; Schulman, T. M.; Manus, M. M. *J. Am. Chem. Soc.* **1974**, *96*, 17.

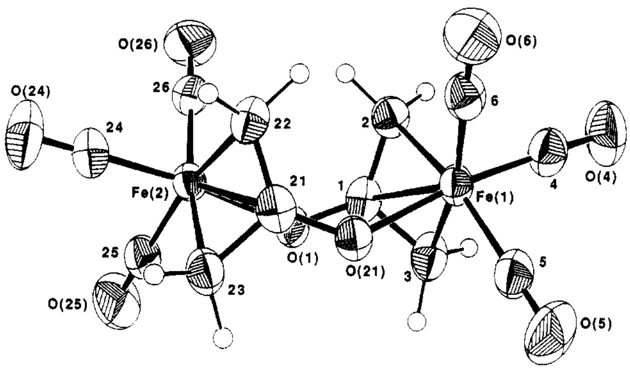

Figure 2. ORTEP drawing of [tricarbonyl(oxodimethylidenemethane)iron]dimer **9**.

Scheme IV

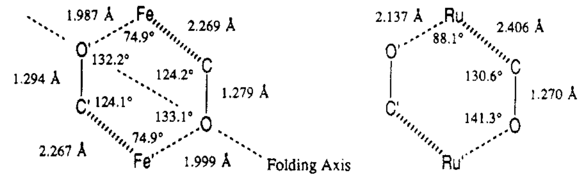

9 **10b**

Table VI. Selected Bond Angles (deg)

C(1)-Fe(1)-C(2)	37.9 (2)	C(21)-Fe(2)-C(22)	37.2 (2)
C(1)-Fe(1)-C(3)	37.9 (2)	C(21)-Fe(2)-C(23)	38.1 (2)
C(2)-Fe(1)-C(3)	68.0 (2)	C(22)-Fe(2)-C(23)	67.8 (2)
C(1)-Fe(1)-C(21)	74.9 (2)	C(21)-Fe(2)-C(1)	74.9 (2)
C(2)-Fe(1)-O(21)	96.0 (2)	C(22)-Fe(2)-O(1)	95.4 (2)
C(3)-Fe(1)-O(21)	88.3 (2)	C(23)-Fe(2)-O(1)	88.3 (2)
C(4)-Fe(1)-O(21)	173.0 (2)	C(24)-Fe(2)-O(1)	173.4 (2)
C(5)-Fe(1)-O(21)	83.5 (2)	C(25)-Fe(2)-O(1)	83.3 (2)
C(6)-Fe(1)-O(21)	93.7 (2)	C(26)-Fe(2)-O(1)	92.7 (2)
C(1)-Fe(1)-C(4)	105.8 (2)	C(21)-Fe(2)-C(24)	104.8 (2)
C(2)-Fe(1)-C(4)	88.3 (2)	C(22)-Fe(2)-C(24)	87.8 (2)
C(3)-Fe(1)-C(4)	88.3 (3)	C(23)-Fe(2)-C(24)	87.7 (2)
C(1)-Fe(1)-C(5)	126.2 (2)	C(21)-Fe(2)-C(25)	127.2 (2)
C(2)-Fe(1)-C(5)	162.1 (3)	C(22)-Fe(2)-C(25)	162.8 (2)
C(3)-Fe(1)-C(5)	94.2 (2)	C(23)-Fe(2)-C(25)	95.1 (2)
C(4)-Fe(1)-C(5)	90.7 (2)	C(24)-Fe(2)-C(25)	91.9 (2)
C(1)-Fe(1)-C(6)	128.0 (2)	C(21)-Fe(2)-C(26)	128.6 (2)
C(2)-Fe(1)-C(6)	96.3 (2)	C(22)-Fe(2)-C(26)	97.7 (2)
C(3)-Fe(1)-C(6)	164.0 (2)	C(23)-Fe(2)-C(26)	165.5 (2)
C(4)-Fe(1)-C(6)	91.3 (3)	C(24)-Fe(2)-C(26)	92.5 (3)
C(5)-Fe(1)-C(6)	101.6 (3)	C(25)-Fe(2)-C(26)	99.5 (3)
C(1)-O(1)-Fe(2)	133.1 (3)	C(21)-O(21)-Fe(1)	132.2 (3)
Fe(1)-C(1)-O(1)	124.2 (3)	Fe(2)-C(21)-O(21)	124.1 (3)
Fe(1)-C(1)-C(2)	65.3 (2)	Fe(2)-C(21)-C(22)	66.6 (2)
O(1)-C(1)-C(2)	126.3 (4)	O(21)-C(21)-C(22)	126.4 (4)
Fe(1)-C(1)-C(3)	66.0 (3)	Fe(2)-C(21)-C(23)	66.5 (3)
O(1)-C(1)-C(3)	119.6 (4)	O(21)-C(21)-C(23)	118.1 (5)
C(2)-C(1)-C(3)	112.1 (4)	C(22)-C(21)-C(23)	113.8 (4)
Fe(1)-C(2)-C(1)	76.8 (3)	Fe(2)-C(22)-C(21)	76.2 (3)
Fe(1)-C(3)-C(1)	76.1 (3)	Fe(2)-C(23)-C(21)	75.5 (3)
Fe(1)-C(4)-O(4)	178.3 (6)	Fe(2)-C(24)-O(24)	178.6 (6)
Fe(1)-C(5)-O(5)	178.8 (6)	Fe(2)-C(25)-O(25)	178.3 (6)
Fe(1)-C(6)-O(6)	178.4 (5)	Fe(2)-C(26)-O(26)	178.3 (5)

the source temperature and neither with the probe-tip temperature nor the ionization energy (cf. Figure 3, supplementary material (see paragraph at end of paper)). At source temperatures above 200 °C, the peak intensities of **6** and its fragments predominate the mass spectrum of **13b**. Further heating leads to the appearance of additional peaks that have not yet been identified. The bromo complex **13a** shows the same behavior, although less pronounced.

X-ray Molecular Structure of (Oxyallyl)iron Complex 9. The molecular geometry and atom-numbering system of **9** are shown in Figure 2, while Tables IV–VI summarize the results obtained. The compound clearly represents a dimer of **6** with a slightly distorted C_2 geometry, in complete agreement with the structure found in solution. The deviations from the ideal symmetry may be a result of packing effects in the crystal lattice. The central part of the complex consists of a folded six-membered heterocyclic ring. All distances between the ring members across this ring lie far beyond bonding interactions, indicated in Table V by dotting separations. The folded ring conformation arises as a consequence of the small interligand angle at the iron centers combined with a valence angle at the oxygen atoms, somewhat above the range[23] of aromatic ether links (Scheme IV). The related ruthenium complex **10b** shows a flat inner skeleton (defined by the six-membered heterocyclic ring Ru–O′– C′(1)–Ru′–O–C(1) at the expense of an unusually large valence angle at the oxygen atoms.

The oxyallyl ligands do not have a flat skeleton: the oxygen atoms are bent toward the metal by 13.6° and 13.7° out of the plane defined by the three allylic carbon atoms. Similar values are found[24] in **18** (12.2°) and **19** (12.9°). Although a tilt angle τ[25] has been introduced in the literature[26] for the description of allylic complexes, the folding angle[27] in the four-membered ring structure, consisting of the three allylic carbon atoms and the metal center, seems to be far more appropriate for a discussion of structural changes. The folding angles found in **9** (60.4° and 60.7°) are clearly smaller than the value found in **17** but still considerably larger compared with the iridium complex **19** (cf. Table III), in full agreement with the midway position of **9** between allylic and metallacyclobutanone structures as concluded from the measured $^1J_{C,H}$ coupling constants.

The observed bond lengths also support this explanation: the C–O bond length (1.294 and 1.279 Å, respectively) of the two somewhat different oxyallyl ligands is definitely longer compared to a free ketone function (1.20 Å) but slightly shorter than a C–O single bond.[28] X-ray structures of allylic iron complexes with σ-donating ketone ligands for a comparison are rare. Tricarbonyl[1–3-η-5-oxo-2-hexenyl-*O*]iron hexafluorophosphate, **20**,[29] an intermediate of Friedel–Crafts acylation of (η^4-butadiene)tricarbonyliron, representing such a case, shows despite the complexation by iron, nearly undisturbed ketone function (C–O bond length 1.207 Å). It therefore fits, that the corresponding Fe···O distance (1.999 Å) in **20** lies just above the average of the Fe···O bond lengths in complex **9** (1.987 and 1.999 Å). It should be noted, however, that all the distances between iron and its ligands in complex **20** exceed the corresponding distances in complex **9**.

Conclusion

The title complex **9** at close examination reveals an important structural link between the classical π-allylmetal complex type and the very recently known metallacyclo-

---

[23] Abrahams, S. C. *Q. Rev., Chem. Soc.* **1956**, *10*, 407.

[24] (a) Cambridge Crystallographic Data Base, Jan release 1989. (b) Allen, F. H.; Kennard, O.; Taylor, R. *Acc. Chem. Res.* **1983**, *16*, 146.

[25] Angle between the plane defined by the allylic carbon atoms and the vector connecting the metal atom with the center of gravity of the allylic ligand.

[26] Kaduk, J. A.; Poulos, A. T.; Ibers, J. A. *J. Organomet. Chem.* **1977**, *127*, 245.

[27] Considering folding along the line connecting the terminal allylic carbon atoms.

[28] C–O bond lengths depend on hybridization of the carbon atom: C(sp^3)–O 1.41 Å, C(sp^2)–O 1.34 Å.

[29] Hardy, A. D. U.; Sim, G. A. *J. Chem. Soc., Dalton Trans.* **1972**, 2305.

butanone compounds with σ-type metal carbon bonds. The high acidity of the hydroxyl function in complex **13a** suggests this "in between" structural position to be more general and not restricted to one particular compound. Whether this conclusion applies also for π-allyl complexes without a substituent at the central carbon has not yet been examined. In contradiction to the classical MO description of π-allyl complexes, a nucleophilic reactivity would be predicted for the central carbon in this case.

The striking difference between the monomeric structure of TMM–Fe(CO)$_3$ (**5**) and the dimeric composition of its oxygen analogue **9** may be explained on one hand by the gain in energy from the Fe–O bond formation and, more importantly, on the other hand by the loss of resonance energy as a consequence of the reduced symmetry of the hypothetical monomeric complex **6** compared with the TMM case.

Experimental Section

All manipulations were performed under dry nitrogen atmosphere using standard Schlenk techniques. Solvents were nitrogen saturated and dried according to standard procedures. Compounds **11a**,[8] **11b**,[8] **14**,[30] **17**,[19] **18**,[20] and **19**[21] were prepared by literature methods. Other reagents were used as obtained from commercial sources. Melting points were determined by using a Kofler microapparatus (Reichert Thermovar). Infrared spectra were measured on a BOMEM DA3 FTIR spectrometer. ^{1}H NMR and ^{13}C NMR spectra were recorded on a Bruker AM 360 at 360.13 and 90.56 MHz, respectively. Mass spectra were taken in a VG 70/70E instrument with EI ionization at a source temperature of 180 °C and 64-eV ionization energy unless stated otherwise.

Preparation of 9. A solution of pyridine (606 mg, 7.7 mmol) in diethyl ether (50 cm^3) was added to a solution of AgBF$_4$ (1.49 g, 7.7 mmol) in diethyl ether (100 cm^3) at room temperature to yield a colorless precipitate. To this mixture, a solution of **13a** (1.04 g, 3.8 mmol) in diethyl ether (50 cm^3) was added over 40 min. The resulting solution was filtered immediately after through a plug of silica gel, and the solvent evaporated at room temperature. The crude greenish yellow product (588 mg) was dissolved in a minimum amount of CH$_2$Cl$_2$ at room temperature and cooled to −78 °C to give pure **9** (0.40 g, 1.02 mmol, yield 54%).

9: mp 108 °C (dec); IR (KBr, cm^{-1}) ν(C≡O) 2093 (vs), 2082 (vs), 2011 (vs), 1982 (vs), ν(C–O) 1514 (vs); ^{1}H NMR intensity) 298 K) δ 2.77 (br s, 4 H, H$_{syn}$), 1.70 (br, s, 4 H, H$_{anti}$), (CD$_2$Cl$_2$, 298 K) δ 2.88 (br s, 4 H, H$_{syn}$), 2.15 (br s, 4 H, H$_{anti}$), (CD$_2$Cl$_2$, 223 K) δ 2.88 (br s, 4 H), 2.36 (br s, 2 H), 1.95 (br s, 2 H); ^{13}C NMR (C$_6$D$_6$, 298 K) δ 209.6 (s, C≡O$_{ap}$), 207.9 (s, C≡O$_{eq}$), 168.0 (s, C–O), 44.6 (br, CH$_2$), (CD$_2$Cl$_2$, 223 K) 209.1 (s, C≡O$_{ap}$), 208.1 (s, C≡O$_{eq}$), 207.0 (s, C≡O$_{eq}$), 168.0 (s, C–O), 48.8 (t, $^1J_{CH}$ = 153 Hz, CH$_2$), 39.5 (t, $^1J_{CH}$ = 153 Hz, CH$_2$); MS (rel intensity 392 (0.1, M$^+$), 364 (18.9), 336 (58.8), 308 (67.7), 280 (5.2), 252 (12), 224 (100), 196 (16.3), 168 (21.4), 140 (5.4), 112 (21.8). Anal. Calcd for C$_{12}$H$_8$Fe$_2$O$_8$: C, 36.76; H, 2.04. Found: C, 36.41; H, 2.02.

Pyrolysis of 9 in the Presence of Furan. **9** (100 mg, 0.255 mmol) was placed in a quartz tube held horizontally in an electrical oven. The outlet of the tube was connected via a trap, immerged in liquid nitrogen, to a diffusion pump. The inlet of the tube was separated from a furan reservoir by a needle valve. The apparatus was evacuated, and the temperature raised to 350 °C within 30 min and maintained at that temperature for 1 h. Simultaneously a total of 60 mL of furan was passed through the tube. The material deposited in the trap was then allowed to warm to room temperature, and excess furan evaporated. Analysis of the residue by ^{1}H NMR showed no trace of cycloadduct.

3-Bromo-2-(trimethylsiloxy)-1-butene (11c). Following the procedure of Sakurai,[8] **11c** was prepared in 18.5% overall yield starting from 2-bromopropionic acid. The reaction mixture, after the addition of (CH$_3$)$_3$SiCH$_2$MgCl at −78 °C, was quenched at −30 °C with aquous NH$_4$Cl before warming to room temperature.

11c: Colorless liquid, bp 65 °C/12 mmHg; ^{1}H NMR (C$_6$D$_6$) δ 4.25 (q, ^3J = 6.8 Hz, 1 H, CHBr), 4.16 (d (AB system), $^2J_{ab}$ = 1.6 Hz, 2 H, CH$_2$), 4.01 (d (AB system), $^2J_{ab}$ = 1.6 Hz, 2 H, CH$_2$), 1.55 (d, ^3J = 6.8 Hz, 3 H, CH$_3$), 0.17 (s, 9 H, Si(CH$_3$)$_3$); ^{13}C NMR (C$_6$D$_6$) δ 158.5 (s, C(2)), 90.9 (t, C(1)), 49.9 (d, C(3)), 23.6 (q, C(4)), 0.03 (q, Si(CH$_3$)$_3$); IR (film, cm^{-1}) 2970 (s), 2930 (w), 2900 (w), 1725 (s), 1630 (vs).

Preparation of 13a. Fe$_2$(CO)$_9$ (28.7 g, 78.9 mmol) and **11a** (8.23 g, 39.4 mmol) in benzene (20 cm^3) were stirred at 35 °C during 3 days. Filtration, evaporation of benzene and Fe(CO)$_5$, and chromatography of the residue on silica gel with diethyl ether followed by crystallization in CH$_2$Cl$_2$ at −78 °C yields 4.30 g (15.5 mmol, 39.4%) of pure **13a**.

13a: mp 100 °C (dec); IR (KBr, cm^{-1}) ν(C≡O) 2094 (vs), 2029 (vs), 2002 (vs), ν(C–O) 1352 (vs); ^{1}H NMR (C$_6$D$_6$) δ 3.36 (br s, 1 H, OH), 3.29 (m,[31] 2 H, H$_{syn}$), 3.10 (m,[31] 2 H, H$_{anti}$), (CDCl$_3$) δ 4.8 (br s, 1 H, OH), 4.25 (br d, 2 H, H$_{syn}$), 3.36 (br d, 2 H, H$_{anti}$); ^{13}C NMR (C$_6$D$_6$, 298 K) δ 207.0 (s, C≡O$_{ap}$), 206.5 (s, C≡O$_{eq}$), 148.1 (s, C(2)), 51.4 (dd,[32] $^1J_{C,H}$ = 165.0, 157.5 Hz, C(1,3)); MS (rel intensity) 276/278 (0.3, M$^+$), 248/250 (23), 220/222 (99), 196 (25), 192/194 (64), 168 (64), 140 (47), 112 (23). Anal. Calcd for C$_6$H$_5$FeBrO$_4$: C, 26.01; H, 1.81. Found: C, 26.07; H, 1.83.

Dehydrohalogenation of 13a in Neat Furan. A solution of 48.2 mg (0.609 mmol) pyridine in diethyl ether (4 cm^3) was added to a solution of 118.7 mg (0.609 mmol) of AgBF$_4$ in diethyl ether (8 cm^3) to yield a colorless precipitate which was allowed to settle. The diethyl ether was decanted and the residue suspended in furan (4 cm^3). To this suspension a solution of 83.4 mg (0.301 mmol) of **13a** in furan (4 cm^3) was added. After filtration through a plug of Celite, the furan was evaporated. The residue contained 20.5 mg of **9** (0.052 mmol, yield 35%) but no trace of the furan cycloadduct **15a**.

Pyrolysis of 13a. **13a** (330 mg, 1.2 mmol) was heated in a FVP apparatus[33] to 400 °C. The volatile products were trapped on a coldfinger and transferred to the fused-on NMR tube. Propanone (19.3 mg, 0.33 mmol, yield 28%) was identified as the only product by ^{1}H NMR using toluene as an internal standard.

Propanone: ^{1}H NMR (C$_6$D$_6$) δ 1.62 (s, 6 H, CH$_3$); ^{13}C NMR (C$_6$D$_6$) δ 204.0 (s, CO), 30.1 (s, CH$_3$).

Preparation of 13b. **11b** (4.52 g, 27.5 mmol) and Fe$_2$(CO)$_9$ (20 g, 55 mmol) in benzene (20 cm^3) were stirred at 35 °C during 5 days. Filtration and evaporation of benzene and Fe(CO)$_5$ gave 3 g of a mixture of **12b** and **13b**. Chromatography of this mixture on silica gel with diethyl ether followed by crystallization from CH$_2$Cl$_2$ at −78 °C yielded 0.429 g (1.85 mmol, 6.7%) of pure **13b**.

12b: ^{1}H NMR (C$_6$D$_6$) δ 3.36 (br s, 1 H, OH), 3.29 (m,[31] 2 H, H$_{syn}$), 3.10 (m,[31] 2 H, H$_{anti}$), 0.09 (s, 9 H, Si(CH$_3$)$_3$).

13b: mp 96 °C (dec); IR (KBr, cm^{-1}) ν(C≡O) 2094 (vs), 2029 (vs), 2004 (vs) ν(C–O) 1352 (vs); ^{1}H NMR (C$_6$D$_6$) δ 3.71 (br s, 1 H, OH), 3.37 (br s, 2 H, H$_{syn}$), 2.98 (br s, 2 H, H$_{anti}$); ^{13}C NMR (C$_6$D$_6$, 272 K) δ 205.2 (s, C≡O$_{eq}$), 204.7 (s, C≡O$_{ap}$), 148.1 (s, C(2)), 54.3 (dd,[34] $^1J_{C,H}$ = 167, 158 Hz, C(1,3)); MS (rel intensity) 206/204 (15, M$^+$ − CO), 197 (25), 196 (35), 178/176 (75), 169 (95), 168 (80), 150/148 (80), 141 (50), 140 (60), 113 (100), 112 (35). Anal. Calcd for C$_6$H$_5$FeClO$_4$: C, 30.99; H, 2.15. Found: C, 30.24; H, 2.15.

Attempted Reaction of 14 with Fe$_2$(CO)$_9$. **14** (4.2 g, 25.5 mmol, containing 2% **11b** even after careful distillation) and Fe$_2$(CO)$_9$ (1.3 g, 3.5 mmol) were stirred without solvent for 3 days at room temperature. After workup, traces of **12b** and **13b** were detected by ^{1}H NMR. These products arise from the **11b** contamination, since the recovered **14** (4.1 g), now exempt of **11b**, was resubjected to the reaction conditons and did not yield any further traces of products. Continued heating of the slurry resulted only in decomposition of the Fe$_2$(CO)$_9$ and partial formation of Fe$_3$(CO)$_{12}$. No products were observed either by photolysis of **14** with Fe(CO)$_5$ in THF at lower temperatures or exposure to Na$_2$Fe(CO)$_4$.

Preparation of 15a. A suspension of 5.15 g (37.8 mmol) of ZnCl$_2$ and 3.11 g (18.9 mmol) of **11b**[8] in a mixture of 16.2 g (238 mmol) of furan and CH$_2$Cl$_2$ (20 cm^3) was stirred at room temperature for 21 days. The dark suspension was filtered and washed several times with aqueous EDTA solution and the organic layer

---

[30] Poirier, J.-M.; Hennequin, L. *Synth. Commun.* **1985**, *15*, 217.

[31] Part of AA′XX′ system, cf. Table I for coupling constants.

[32] Coupling constants were determined in CDCl$_3$ at 263 K.

[33] Williams, D. J.; Pearson, J. M.; Levy, M. *J. Am. Chem. Soc.* **1970**, *92*, 1436.

[34] Coupling constants were determined in CDCl$_3$ at 273 K.

dried over $MgSO_4$. Evaporation of the solvent and destillation in a Kugelrohr apparatus yielded 278 mg of a 1:1 mixture (determined by ^1H NMR) of **15a** (5.9%) and 1-(2-furanyl)propan-2-one (5.9%).

1-(2-Furanyl)propan-2-one: ^1H NMR (C_6D_6) δ 6.99 (dd, ^3J = 2.3 Hz, ^4J = 0.4 Hz, 1 H, H–C(5′)), (dd, ^3J = 3.3 Hz, ^3J = 2.3 Hz, 1 H, H–C(4′)), 5.92 (dd, ^3J = 3.3 Hz, ^4J = 0.4 Hz, 1 H, H–C(3′)), 3.84 (s, 2 H, H–C(1)), 1.65 (s, 3 H, H–C(3)).

15a: ^1H NMR (C_6D_6) δ 5.54 (s, 2 H, H–C(6,7)), 4.42 (d, 2 H, ^3J = 5.1 Hz, H–C(1,5)), 2.29 (dd (AB system), $^2J_{ab}$ = 16.8 Hz, ^3J = 5.1 Hz, 2 H, H_{exo}–C(2,4)), 1.91 (dd (AB system), $^2J_{ab}$ = 16.8 Hz, ^3J = 0.6 Hz, 2 H, H_{endo}–C(2,4)).

Preparation of 15b. A suspension of 3.0 g (22 mmol) of $ZnCl_2$ and 2.45 g (11 mmol) of **11d** in a mixture of 9.4 g (138 mmol) of furan and CH_2Cl_2 (20 cm^3) was stirred at room temperature for 11 days to give 750 mg (5.5 mmol, yield 50%, after the same workup as described for **15a**) of **15b** consisting of an endo:exo mixture of 73.6:26.4, as determined by ^1H NMR.[35]

***endo*-15b**: ^1H NMR (C_6D_6) δ 5.71 (dd (AB system), $^2J_{ab}$ = 6.0 Hz, ^3H = 1.7 Hz, 1 H, H–C(7)), 5.65 (dd (AB system), $^2J_{ab}$ = 6.1 Hz, ^3J = 1.7 Hz, 1 H, H–C(6)), 4.46 (ddd, ^3J = 4.9 Hz, ^3J = 1.7 Hz, ^3J = 1.1 Hz, 1 H, H-C(5)), 4.40 (dd,^3J = 4.7 Hz, ^3J = 1.7 Hz, 1 H, H–C(1)), 2.36 (qd, ^3J = 7.1, ^3J = 4.7 Hz, 1 H, H_{exo}–C(2)), 2.32 (dd (AB system), $^2J_{ab}$ = 15.6 Hz, ^3J = 4.9 Hz, 1 H, H_{endo}–C(4)), 1.93 (dd (AB system), $^2J_{ab}$ = 15.6 Hz, ^3J = 1.1 Hz, 1 H, H_{exo}–C(4)), 0.75 (d, ^3J = 7.1 Hz, 3 H, H–C(2^1)); ^{13}C NMR ($CDCl_3$) δ 206.7 (s, C(3)), 134.5 and 131.5 (d, C(6,7)), 81.4 and 77.8 (d, C(1,5)), 51.2 (d, C(2)), 45.6 (t, C(4)), 9.8 (q, C(2^1)).

***exo*-15b**: ^1H NMR (C_6D_6) δ 5.63 (dd (AB system), $^2J_{ab}$ = 6.0 Hz, ^3J = 1.7 Hz, 1 H, H–C(7)), 5.59 (dd (AB system), $^2J_{ab}$ = 6.0 Hz, ^3J = 1.7 Hz, 1 H, H–C(6)), 4.40 (br d, ^3J = 5.1 Hz, 1 H, H–C(1)), 4.15 (br, 1 H, H–C(5)), 2.39 (ddd (AB system), $^2J_{ab}$ = 16.3 Hz, ^3J = 5.1 Hz, ^4J = 0.9 Hz, 1 H, H_{exo}–C(4)), 1.98 (qq, ^3J = 7.4, ^3J = 0.9 Hz, ^4J = 0.9 Hz, ^4J = 0.9 Hz, 1 H, H_{endo}–C(2)), 1.83 (dt (AB system), $^2J_{ab}$ = 16.3 Hz, ^3J = 1.0 Hz, ^4J = 0.9 Hz, 1 H, H_{endo}–C(4)), 1.12 (d, ^3J = 7.4 Hz, 3 H, H–C(2^1)); ^{13}C NMR ($CDCl_3$) δ 208.9 (s, C(3)), 133.3 and 133.2 (d, C(6,7)), 81.8 and 77.0 (d, C(1,5)), 50.0 (d, C(2)), 44.1 (t, C(4)), 15.5 (q, C(2^1)).

X-ray Analysis of 9. Suitable crystals, in the form of orange hexagonal plates, were grown from toluene. A crystal of dimensions 0.38 × 0.29 × 0.09 mm was used for data collection. Preliminary Weissenberg and precission photographs indicated the crystals to be orthorhombic, space group *Pbcm* or $Pbc2_1$.[36] Intensity data, with index limits *h* 0–15, *k* 0–8, *l* 0–26 and θ_{max} = 27.5°, were measured on a Stoe Siemens AED2 four-circle diffractometer (graphite-monochromated Mo Kα radiation) using the ω/θ scan mode at room temperature (295 K). The intensity variation for four standard reflections measured every hour was ca. 3%. Of the 1660 unique reflections measured, 1442 were considered observed ($F_o > 4\sigma(F_o)$). Cell parameters from $\pm\omega$ values of 63 reflections in the range of $20° < 2\theta < 30°$. A numerical absorption correction was applied to the intensity data on the basis of the crystal dimensions using the ABSC subroutine in the SHELX-76 program,[37] transmission 0.861–0.585. The structure was solved by direct methods using the program SHELXS-86.[38] The *E* statistics clearly indicated the structure to by acentric, and this was confirmed by the stable refinement. The program SHELX-76 was used for all further calculations. In the final cycles of least-squares refinement the H atoms were included in idealized positions with an overall isotropic thermal parameter (refined value 0.0663 Å^2). Weighted anisotropic full-matrix least-squares refinement for 1440 reflections (two reflections probably suffering from extinction were removed) converged at *R* = 0.028, *R* = 0.031 with $w^{-1} = \sigma^2(F_o) + 0.00115(F_o^2)$. Parameter shift/esd 0.024 (maximum), < 0.01 (average). Heights in final difference map $\Delta\rho_{max}$ = 0.30, $\Delta\rho_{min}$ = –0.32 e Å^{-3}. Atomic scattering factors were taken from ref. 39. Final positional and equivalent isotropic thermal parameters are given in Table V, bond distances and angles in Table VI. The crystallographic numbering scheme is apparent from Figure 2, prepared by using ORTEP-II.[40]

Acknowledgment. F. Nydegger is thanked for measuring the mass spectra. This work was supported by the Swiss National Science Foundation (Grant No. 20-5112.86), which is gratefully acknowledged. H.S.-E. wishes to thank the Swiss National Science Foundation for an equipment grant (No. 2.372-0.84).

Supplementary Material Available: EI mass spectra of **13b** (1 page); a listing of observed and calculated structure factors for **9** (9 pages). Ordering information is given on any current masthead page.

---

[35] Assignment of the endo structure to the main isomer was made possible through the observation of mutual nOe's between the signal of the methyl group at 0.75 ppm and the signals of the protons at C(1) and C(7), and the endo proton at C(4).

[36] $Pbc2_1$ is an alternate setting of the space group $Pca2_1$, which appears in the *International Tables*.

[37] Sheldrick, G. M. SHELX-76, *Program for Crystal Structure Determination*; University of Cambridge: UK, 1976.

[38] Sheldrick, G. M. SHELXS-86, *Program for Crystal Structure Determination*; University of Gottingen: German Federal Republic, 1986.

[39] *International Tables for X-ray Crystallography*; Kynoch Press: Birmingham, England, 1974; Vol. IV.

[40] Johnson, C. K. ORTEP-II, Report ORNL-5138; Oak Ridge National Laboratory: Oak Ridge TN, 1974.